In situ remediation of metal(loid)-contaminated lake sediments with alkali-activated blast furnace slag granule amendment: A field experiment

Johanna Laukkanen[1,3] · Esther Takaluoma[2] · Hanna Runtti[3] · Jari Mäkinen[4] · Tommi Kauppila[4] · Seppo Hellsten[5] · Tero Luukkonen[6] · Ulla Lassi[3]

Abstract

Purpose Adsorbent amendment to contaminated sediments is one in situ remediation method to decrease the bioaccessibility of pollutants from the sediments. In this work, alkali-activated blast furnace slag (BFS) granules were used in a field experiment at Lake Kivijärvi (Finland). The lake was heavily affected by a mining accident in 2012, which released a significant peak load of metals and sulfate. The purpose of this work was to evaluate the performance of the novel amendment material for in situ remediation in real conditions with a preliminary cost estimation.

Methods Alkali-activated BFS granules were prepared and characterized for composition, microstructure, and surface properties. Two mesocosms were placed in the lake: one with granule dosing and another without. Sediment and pore water samples were collected after a two-week period. Similar small-scale experiment was performed in laboratory with a three-month duration. Bioaccessibility of metals from sediments was assessed with a three-stage leaching procedure.

Results The granules were effective in decreasing the mobility of Fe, Zn, Ni, and Cr in all leaching stages by approximately 50–90% in comparison with unamended sediment in the mesocosm experiment. Laboratory-scale incubation experiments also indicated decreased release of Ba, Co, Ni, Al, Fe, Mg, Mn and S. The estimated material costs were lower than the removal of the contaminated sediments with dredging and off-site treatment.

Conclusion The results showed preliminarily the effectiveness of alkaline-activated BFS in the remediation of metal-contaminated sediments in a field experiment. However, topics requiring further study are the leaching of trace elements from the material and impact on the sediment pH.

Keywords Active capping · Alkali-activated materials · Blast furnace slag · Geopolymer · Sediment

✉ Johanna Laukkanen
johanna.laukkanen@oulu.fi

1. Kerttu Saalasti Institute, University of Oulu, Pajatie 5, 85500 Nivala, Finland

2. Kajaani University of Applied Sciences, Kuntokatu 5, 87100 Kajaani, Finland

3. Research Unit of Sustainable Chemistry, University of Oulu, 90014 Oulu, Finland

4. Geological Survey of Finland, 70211 Kuopio, Finland

5. Freshwater Centre, Finnish Environmental Institute, 90014 Oulu, Finland

6. Fibre and Particle Engineering Research Unit, University of Oulu, 90014 Oulu, Finland

1 Introduction

Lakes and other water bodies can be adversely affected by unsuccessful mine closure (Ciszewski et al. 2012) or accidental release of untreated effluents and tailings (Cagnin et al. 2017; Saup et al. 2017) due to elevated metal(loid)[1] load. Ultimately, sediments act as the sink of metal(loid)s; however, changes in pH or redox potential may result in re-dissolution of the scavenged contaminants (Calmano et al. 1993; Salomons and Stigliani 2012). In such cases, the sediments become a source of secondary pollution and increase the potential bioaccessibility of metals.

---

[1] The term metal(loid) is used in this article to cover metals and metalloids. (Sometimes they are also referred to as potentially toxic elements or heavy metals.).

To minimize the risk of metal(loid) re-dissolution, in situ remediation by active capping or sediment augmentation with adsorbents has been studied as a less disruptive and lower-cost option for dredging and off-site treatment (Zhang et al. 2016). In augmentation, adsorbent material is mixed in the sediment (Alvarado et al. 2020), while in active capping, adsorbent is applied on the sediment surface as a thin, normally few centimeter-thick layer with the aid of geotextiles (Viana et al. 2008; Zhang et al. 2016). In addition to adsorption and other sequestration mechanisms, active capping also provides physical and chemical isolation for the sediment and reduces the flux of dissolved contaminants into the overlying water column (Zhang et al. 2016). Consequently, the potential bioaccessibility of metal(loid)s decreases. Modeling of active capping set-ups has demonstrated that effective metal(loid) stabilization can be achieved for up to 100 years (Viana et al. 2008). Some examples of active capping or augmentation materials for metal(loid) stabilization include limestone, steel slag, activated carbon (with or without chemical modifications), iron sulfide minerals, crushed concrete, bentonite, bauxite, commercial Aquablok® material, organoclay, and apatite (Viana et al. 2008; Dixon and Knox 2012; Randall et al. 2013; Kang et al. 2016; Ting et al. 2018; Park et al. 2019; Ting and Hsi 2019).

Alkali-activated materials (AAMs) could represent another active capping or augmentation material option since they have been successfully used for the removal of a number of aqueous metal(loid)s (e.g., As, Cd, Cr, Co, Cs, Cu, Mn, Ni, Pb, Sb, Sr, and Zn) as summarized by Luukkonen et al. 2019. Furthermore, the use of alkali-activated metakaolin and blast furnace slag (BFS) decreased the potential bioaccessibility of Ni, Zn, Al, Cu, Cr, and Fe in laboratory-scale in situ sediment remediation experiments (Kutuniva et al. 2019). AAMs are hydrous alkali or alkaline-earth metal aluminosilicates with mesoporous and amorphous structures. They are prepared by reacting an aluminosilicate precursor and a high-pH alkali-activator solution under (near) ambient conditions (Provis 2014). Beneficial features of AAMs include the potential to use industrial side-streams as raw materials and a low-energy manufacturing process (Mehta and Siddique 2016). In the case of low-calcium raw materials, the obtained molecular-level structure consists of a three-dimensional network containing SiQ4(2Al) and SiQ4(3Al) environments that resembles zeolites but with a low level of crystallinity (Lecome et al. 2006). When high-calcium raw materials are used, the structure consists of Al-substituted tobermorite-like chains (SiQ2 and SiQ2(1Al) environments) with a varying degree of crosslinking (Lecome et al. 2006; Myers et al. 2013). The removal of cations in AAMs occurs via ion exchange at negatively charged Al sites (e.g., [AlO4]−) (Bortnovsky et al. 2008; Guo and Shi 2017). Anions, on the other hand, can be adsorbed layered double hydroxides, which are secondary reaction products of alkali-activation whose formation is promoted by a high Mg content in high-Ca alkali-activated systems (Parker et al. 1995; Trifiro and Vaccari 2004; Provis and Bernal 2014).

In the present study, high-shear granulation combined with alkali activation was used as a facile and up-scalable manufacturing method for alkali-activated BFS adsorbent granules. The granules were used as a sediment amendment material in a field remediation experiment at Lake Kivi-järvi (Sotkamo, Finland). The present study is the first in which AAMs are used as a sediment amendment material in a field-scale experiment. The performance of the granules was evaluated by sequential leaching experiments and pore water sample collection after two weeks. At the same time, a similar, three-month duration laboratory-scale experiment was performed to support the finding of the field experiment. The results indicate preliminarily that alkali-activated BFS granules have a promising performance in the remediation of metal-contaminated sediments combined with lower costs than dredging and off-site treatment.

2 Materials and methods

2.1 Preparation of alkali-activated granules

Blast furnace slag (Tradename KJ400, Finnsementti, Finland) was used as a precursor for the preparation of alkali-activated granules. Its main characteristics are shown in Table 1. The alkali-activator solution was prepared by mixing 50 wt% NaOH solution (Algol, Finland), 35 wt% sodium silicate solution ($SiO_2/Na_2O = 2.55$, Algol, Finland), and

Table 1 Main characteristics of blast furnace slag (Luukkonen et al. 2016, 2020)

Property and unit	Value
Na_2O [wt%]	0.51
MgO [wt%]	10.24
Al_2O_3 [wt%]	9.58
SiO_2 [wt%]	32.33
P_2O_5 [wt%]	0.01
SO_3 [wt%]	4.00
K_2O [wt%]	0.53
CaO [wt%]	38.51
Fe_2O_3 [wt%]	1.23
Loss on ignition [wt%]	0.46
d_{10} [µm]	0.9
d_{50} [µm]	10.8
d_{90} [µm]	51.7
Bulk density [g cm^{-3}]	1.20
Solid density [g cm^{-3}]	2.93
Specific surface area (by N_2 adsorption) [m^2 g^{-1}]	2.79

water in a weight ratio of 5.0/4.2/1.0, respectively. The alkali-activation-granulation process was performed with a high intensity mixer (R05/T, Eirich, Germany, see Fig. 1A): 25.0 kg of BFS was placed in the mixer, and 10.1 kg of alkali-activator solution was added as batches. The alkali-activation-granulation process was optimized on the basis of alkali-activator solution demand by BFS (i.e., the granules were not too dry or too wet when granulation was finished). The pan was operated in a counter flow current mode at a speed of 15 rpm, and the mixing blades rotated at 315 rpm. The granulation time per batch was 45 s. Granules were sieved to 2–4 mm size, rinsed with water, and stored at ambient conditions until used (Fig. 1B).

2.2 Characterization of blast furnace slag granules

Specific surface area and nanoscale pore size distributions were determined using the Brunauer–Emmett–Teller (BET) isotherm and the Barrett–Joyner–Halenda (BJH) method (i.e., N_2 adsorption–desorption) with Micromeritics ASAP 2020 (USA). The analysis was performed from 1–4-mm granules.

X-ray diffraction (XRD) analysis was performed with a PanAnalytical Xpert Pro diffractometer (Malvern Panalytical, UK) to identify crystalline phases in the AAM. Finely crushed granules were dispersed with ethanol on a glass plate, and the ethanol was allowed to vaporize. Diffractograms were interpreted using Highscore software (version 3.0) and the Crystallography Open Database.

A field-emission scanning electron microscope with an energy dispersive spectroscope (SEM–EDS, Zeiss Ultra Plus, Germany) was used for microstructural imaging and semi-quantitative chemical analysis of the granule top and inner surfaces. The analyses were conducted using a secondary electron detector with 15 kV acceleration voltage and 8.5 mm working distance. The samples were coated with carbon prior to measurement.

Zeta potential measurement was conducted with a Malvern Panalytical instrument. The employed zeta potential transfer standard (ZTS1240, Malvern Panalytical, UK) had a -40 ± 5.8 mV value. Granules were crushed and sieved to less than 0.106 μm particle size for the measurement. 0.1 g of granules and 100 mL of 0.1 M HCl were mixed, and pH was adjusted to approximately 7 to simulate typical pH in the aquatic environment of the lake.

2.3 Characterization of water and sediment samples

The metal concentrations from water samples were analyzed using a PerkinElmer Optima 5300 DV (USA) inductively coupled plasma optical emission spectrometer (ICP-OES). Water samples were acidified prior to analysis by adding 2% (v v^{-1}) nitric acid (65%, Merck Supelco). Sediment samples were digested according to the EPA 3051A method. In short, nitric and hydrochloric acids were added, and a CEM Mars 5X Microwave oven (USA) was used for digestion. The digested samples were filtered and diluted with ultrapure water. The analyses were performed with ICP-OES similarly as mentioned above.

2.4 In situ remediation field experiment

The field experiment took place at Lake Kivijärvi (Sotkamo, Finland). The lake received a significant peak load of metals in 2012 due to a gypsum pond failure at the Talvivaara mine of Terrafame Ltd. (Sotkamo, Finland), located approximately 6 km NE from the lake (Leppänen et al. 2017). More than 240 000 m3 of surface water mixed with untreated process effluent containing 150 t of Fe, 150 t of Mn, 2 t of Ni, 1 t of Zn, 70 kg of U, 60 kg of Co, and 2 kg of Cd was released (Kauppi et al. 2013). The ecological status of Lake Kivijärvi is "passable" due to

Fig. 1 **A** Granulator and **B** appearance of alkali-activated blast furnace slag granules before use
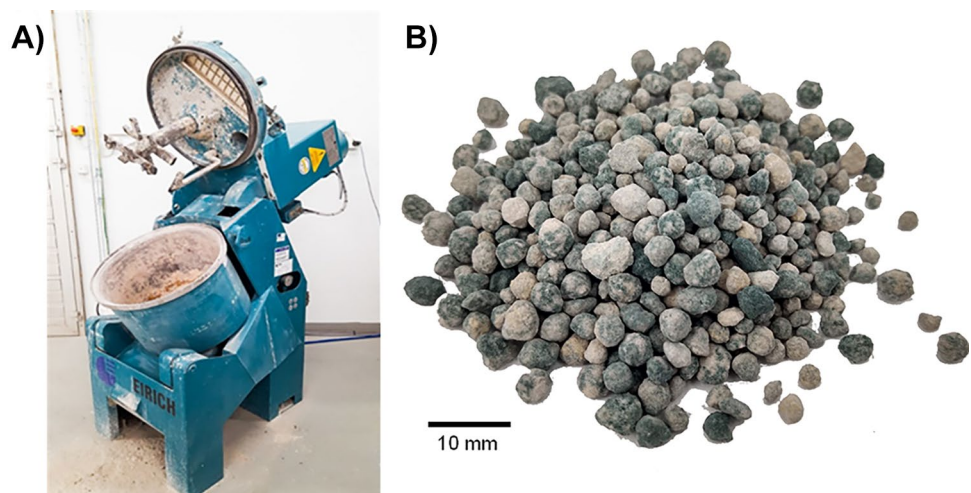
permanent stratification by saline mine waters (Finnish Environment Institute 2019). However, according to the European Union Water Framework Directive, all surface water bodies should achieve a good status by 2027 (European Union 2000). Therefore, efficient measures to restore the natural circulation of waters and to avoid re-dissolution of settled metals are needed (Laamanen et al. 2019).

Two mesocosms (i.e., vinyl acetate tubes with an inner diameter of 1500 mm) were installed with a water depth of approximately 5.5 m (Fig. 2). Both mesocosms were equipped with pumps to enhance circulation in the 5 m water column and break up the stratification caused by the elevated sulfate concentration upon the mining accident. The pumps were used until a complete mixing of the water column was theoretically reached. Ten kilograms of alkali-activated BFS granules were manually spread out in one of the mesocosms and allowed to sink down to the sediment, while the other was left untreated. After two weeks, surface sediment (0–5 cm) samples were taken from both mesocosms with a 60-mm diameter KC Kajak Sediment Core sampler (KC Denmark A/S, Denmark), and the pH of the sediments was measured. At the same time, a similar sediment sample was taken from outside of the mesocosm. The samples were dried at 105 °C and stored in a desiccator until testing. The stability of Al, Fe, Ti, Zn, Ni, Cr, and Cu was studied in amended and unamended sediments. Cd, Co, and U were excluded as their concentrations were low, as also reported in our previous study (Kutuniva et al. 2019). Pore water was collected from the sediments in the field using a disposable vacuum filter with 0.2 µm pore size and conserved with nitric acid. Samples were analyzed with ICP-MS in an accredited laboratory (Labtium Ltd, FINAS 025) employing both laboratory duplicates (every tenth sample and each batch) and certified reference materials.

In conjunction with the mesocosm experiment samples, composite sediment samples were taken from the contaminated sediment layer (0–3 cm) from outside the mesocosms to give a 2 L composite sample. This was used for an incubation experiment in a cold room. In addition, water overlying sediments at the field sites was collected for the incubation experiments. Three types of incubation setups were made in 100-mL plastic vessels: 1) 50 mL of contaminated sediment only, 2) contaminated sediment + 50-mL lake water on top, and 3) contaminated sediment with a BFS layer on top. The vessels were loosely capped with screw caps and placed in a container filled with water, and the whole setup was covered with a plastic film to maintain a high moisture content around the vessels. The setups were kept at 5 °C for three months. Samples were taken from the sediment pore water and lake water before the incubation period and from pore waters and the overlying water of all setups after the experiment and analyzed for metals and DOC.

2.5 Leaching procedure

The sediment samples had total solids of approximately 6.8% when they were collected from the lake. Three different kinds of samples were used in the leaching experiment after drying at 105 °C: 1) sediment without augmentation (blank); 2) sediment with augmentation; and 3) sediment with augmentation, which was ground with a mortar and pestle. Sample '3' was prepared in order to evaluate a scenario in which the granules disintegrate. Each sample was analyzed in triplicate.

The potential bioaccessibility of metals was evaluated by using a three-step sequential leaching method (Rauert et al. 1999). The procedure is shown in Fig. 3. The first step (acid extraction) was performed as follows: a dried sample (0.5 g) and 0.11 M acetic acid (20 mL) were mixed and shaken
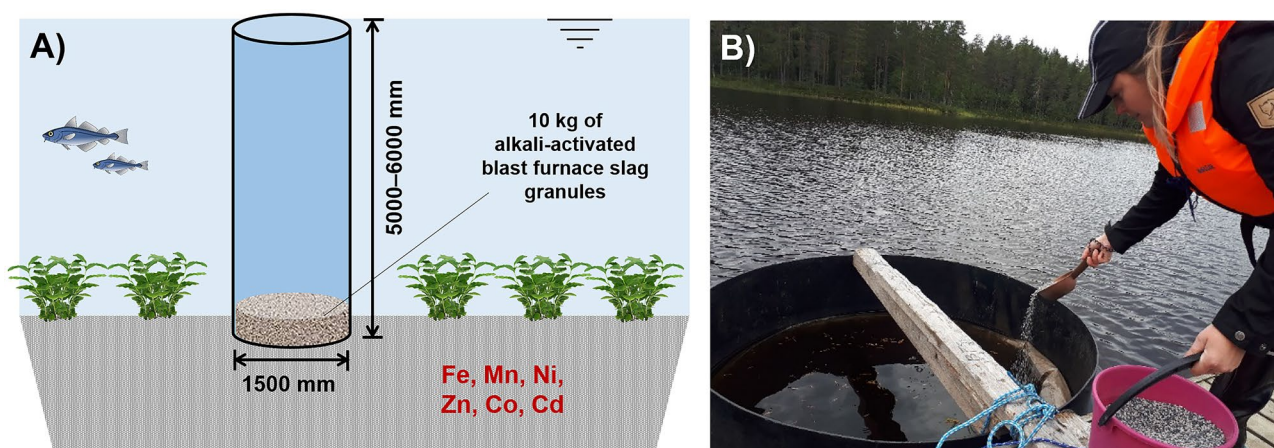
Fig. 2 Experimental setup: **A** schematic presentation of the mesocosm experiment; **B** spreading of alkali-activated blast furnace slag granules to the mesocosm
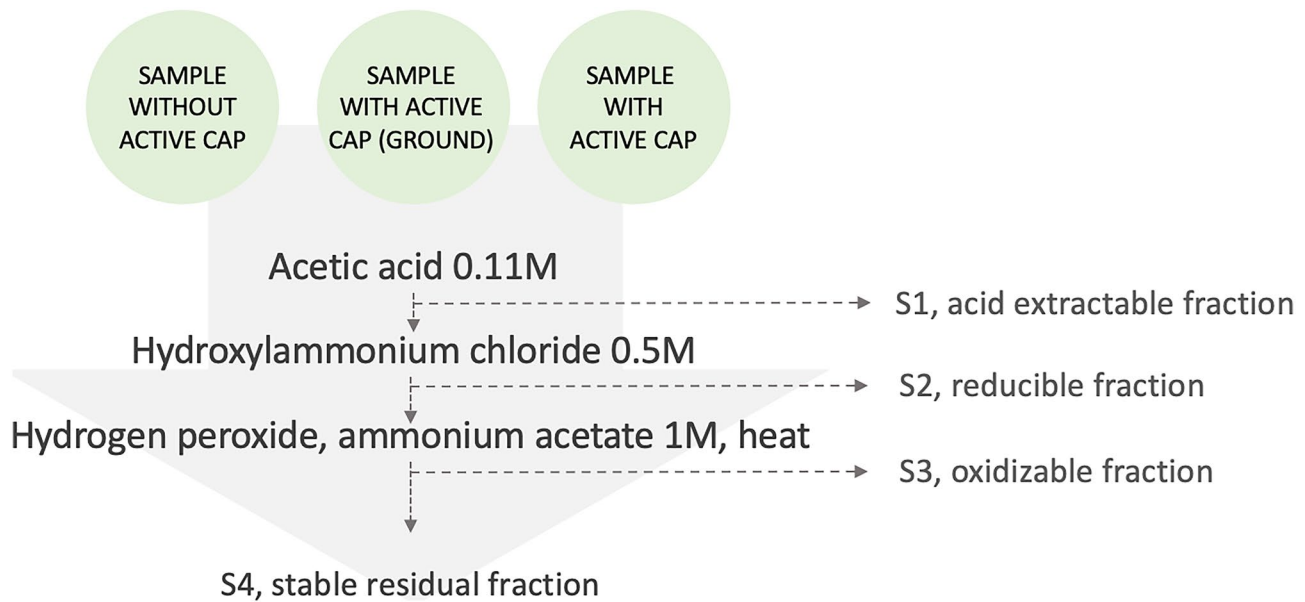
Fig. 3 The procedure of the leaching method

overnight with an end-over-end shaker. After centrifuging, the supernatant solution (S1) was separated and analyzed. The solid residue was mixed with distilled water (10 mL), shaken for 15 min, and separated from water by centrifuging. In the second step (reducing conditions), 0.5 M hydroxylammonium chloride solution (20 mL) was mixed with the solid residue and shaken overnight. The solid residue was then separated by centrifuging, and the supernatant solution (S2) was analyzed. The solid residue was washed with distilled water similarly as described above. In the third step (oxidizing conditions), 5 mL of 30% hydrogen peroxide (VWR Chemicals) was slowly mixed with the solid residue from the second step. The mixture was allowed to react at room temperature for 1 h with occasional shaking. Then, the temperature was increased to 85 °C (in a water bath) for 1 h, and the solution was evaporated to 1.5 mL volume. Another 5 mL of hydrogen peroxide was added, and the volume was evaporated to 0.5 mL. After cooling, 25 mL of 1 M ammonium acetate (VWR Chemicals) solution was added, and the mixtures were shaken overnight. The supernatant (S3) was separated by centrifuging, and the solids were again washed as described above. The final solids (S4) were analyzed as described in Sect. 2.3.

3 Results and discussion

3.1 Characterization of alkali-activated blast furnace slag granules

The micrographs of alkali-activated blast furnace slag granules are shown in Fig. 4. The surface layer has a typical appearance of calcium-aluminum–silicate-hydrate (C-A-S–H) gel with some unreacted plate-like BFS particles and pores. However, the inner parts of granules are essentially nonporous or have only closed porosity. This is also evident from the very low specific surface area (Table 2), which was measured from granules of 1–4-mm diameter. The average composition of the granule surface (as determined by an area analysis in SEM–EDS, Table 3) exhibits a very high concentration of sodium (approx. 41 weight-%), which indicates that the manufacturing process may introduce excessive alkali-activator solution in relation to the BFS weight. The unreacted sodium cations migrate to the surface of granules. In fact, residues of unreacted sodium hydroxide was detected with XRD (see supporting information, Fig. S1). The inner parts of granules were analyzed from crushed samples, and they exhibited more expected sodium content (approx. 9 weight-%).

The zeta potential measurements aimed to characterize the surface sites of the granules. The results revealed two kinds of zeta potential environments, -18.56 ± 1.04 mV and 7.17 ± 1.97 mV, of which the former resulted in a much stronger signal. The negative zeta potential corresponds to the negatively charged C-A-S–H gel (i.e., $[AlO_4]^-$ sites), whereas the smaller peak with positive charge is likely related to the presence of layered double hydroxides.

3.2 Vertical profiles of metals in sediments

The abrupt increase in emissions from the mine site in 2012 are seen at ~2 cm in the chemical profiles as local maxima in concentrations of certain elements (Fig. 5). The vertical
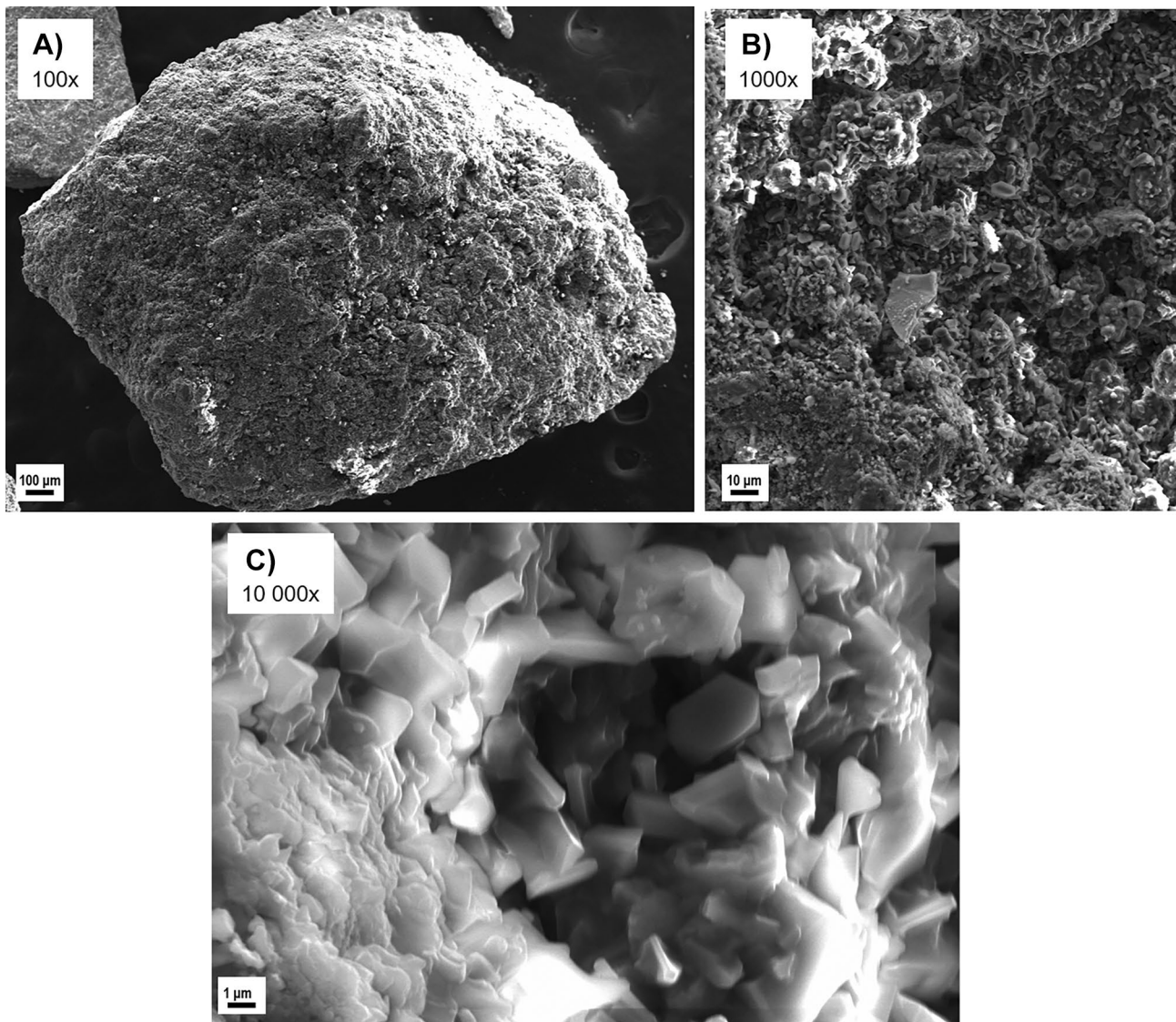
Fig. 4 Micrographs of granule surface: **A** magnification 100x, **B** magnification 1000x, and **C** magnification 10 000x

profile in Fig. 5 is from the sampling location 14 in the northern part of lake Kivijärvi in Laamanen et al. (2019) (also cf. Leppänen et al. 2017). The concentrations of Ni and Zn, in particular, were considerably higher than in the pre-mining sediments. Part of the easily leachable elements (Ca, Mn, Na) has migrated deeper in the sediment profile by

Table 2 Specific surface areas, average pore widths, and cumulative pore volumes of alkali-activated blast furnace slag granules

Parameter	Value
Specific surface area	0.60 m^2 g^{-1}
Average pore width	28.38 nm
Cumulative pore volume	0.0020 cm^3 g^{-1}

Table 3 Average compositions (weight-%) of alkali-activated blast furnace slag granule surface and inner part

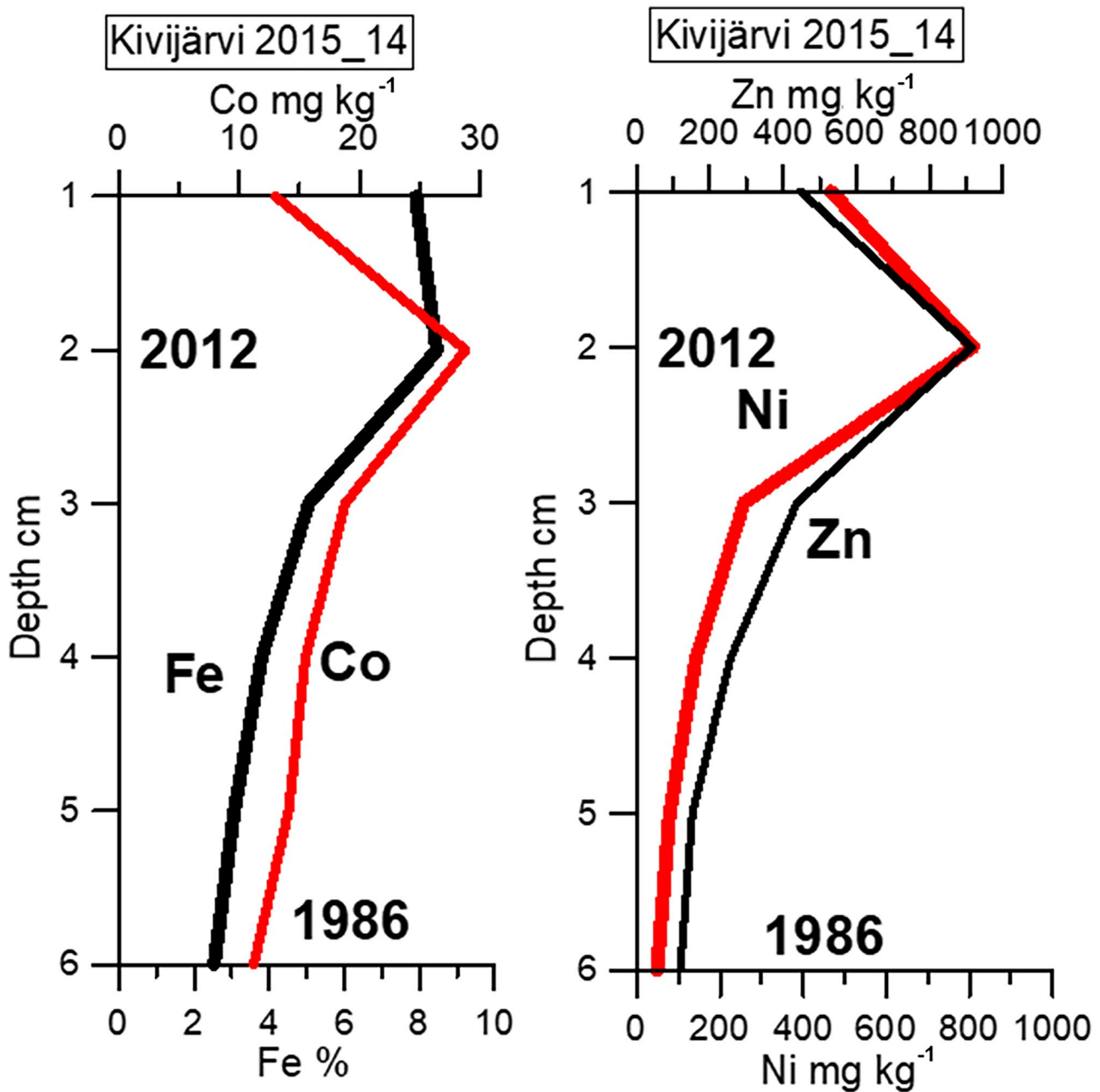| Element [weight-%]	Surface	Inner part
O	53.6	48.9
Na	40.7	9.2
Mg	0.8	3.7
Al	0.4	2.9
Si	1.6	12.0
S	0.2	0.6
K	0.0	0.4
Ca	2.7	22.3
Ti	0.0	0.8

Fig. 5 Vertical profiles of Co, Fe, Zn, and Ni in the sediments. The depth of 6 cm corresponds to year 1986 and the depth of 2 cm to year 2012

diffusion, a feature also seen in the element concentrations of the solid materials (cf. Laamanen et al. 2019).

In addition to changes in the sediment dry matter, mining impacts were seen in the vertical pore water profiles of especially Mn and Ni (a profile taken from immediately outside of the mesocosm). The pore water Mn concentrations have changed to as deep as 30 cm in the sediment, while the changes in pore water Ni were limited to the top 5 cm. In contrast, Zn concentrations in the pore water were stable throughout the vertical profile.

3.3 Performance of alkali-activated granules in the field experiment

The performance of alkali-activated BFS granules in the field experiment was evaluated by the sequential leaching test. Three different kinds of samples were evaluated (after drying): sediment without active cap (blank), sediment with active cap, and sediment with active cap and grinding. The grinding step was included to simulate possible disintegration of the granules in the sediment environment. The results
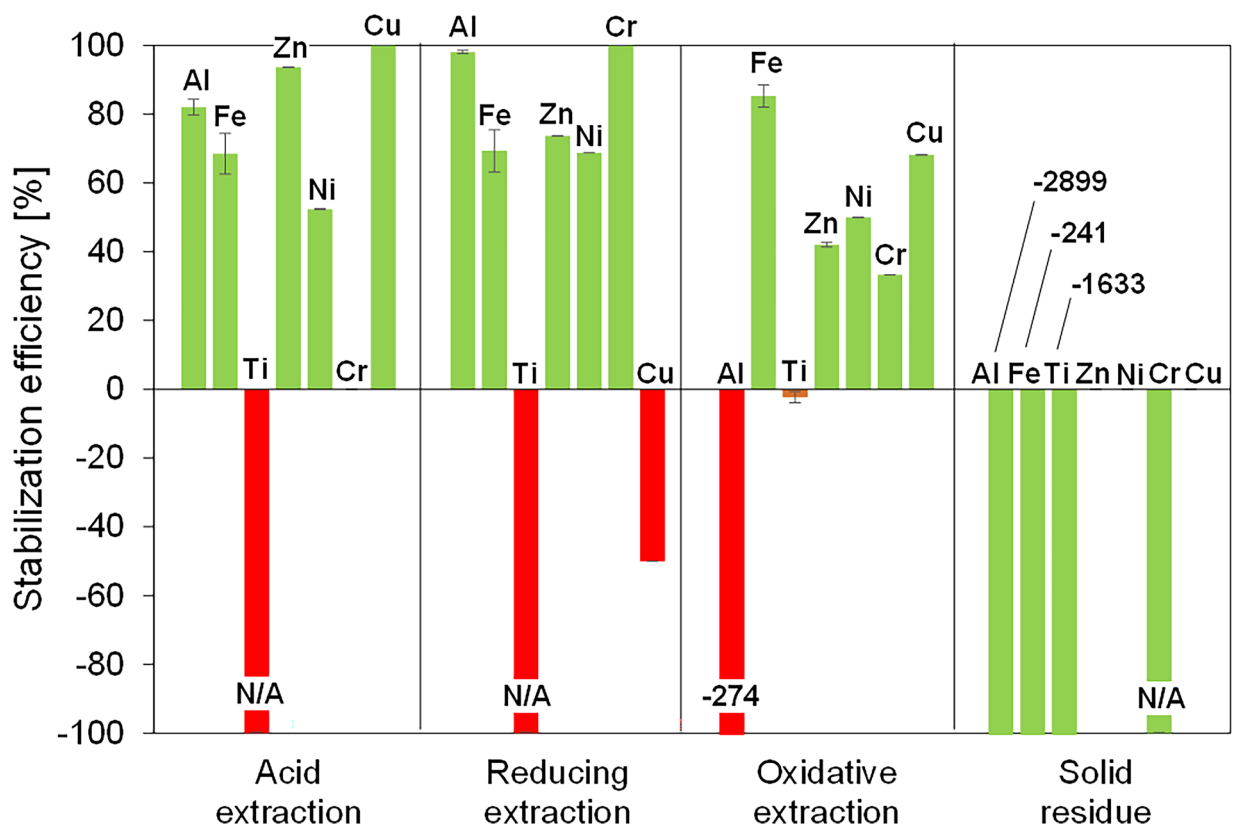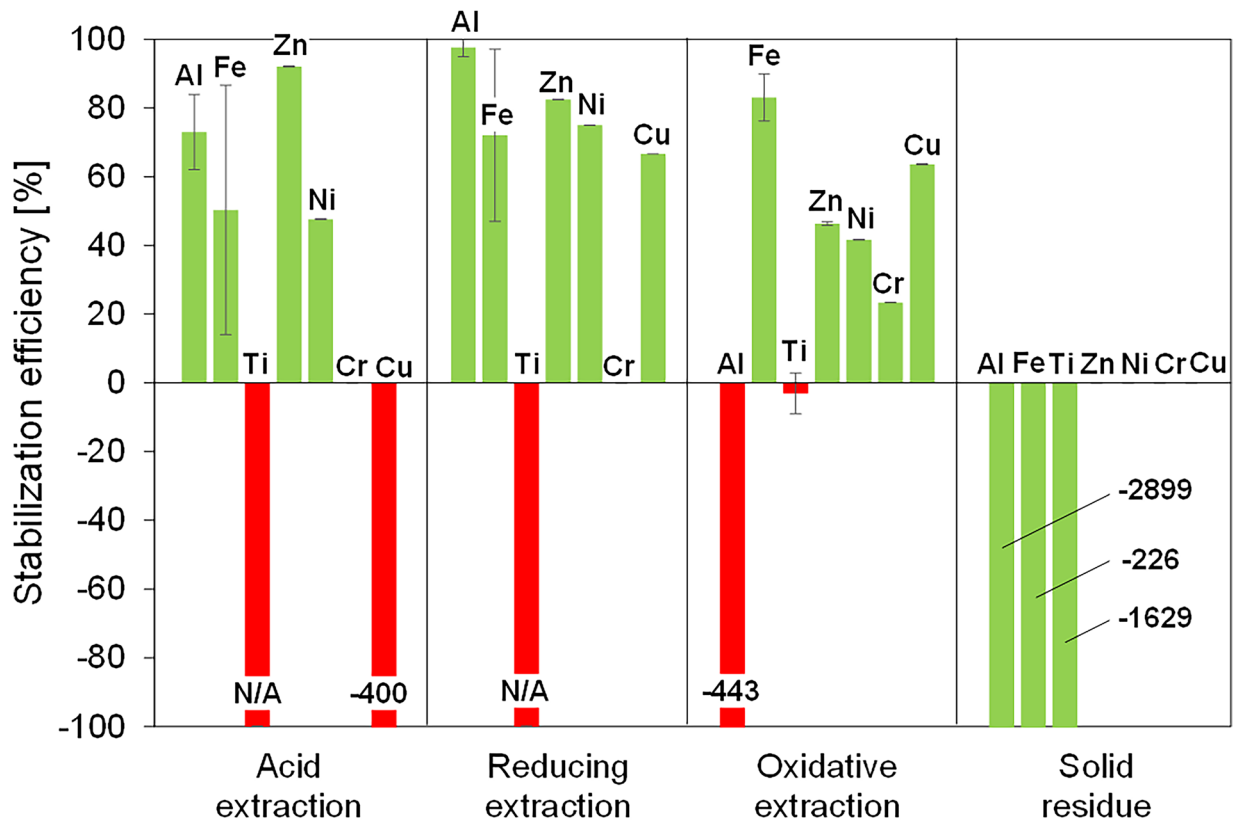
◄**Fig. 6** Results of sequential leaching experiments: **A** sediment and active cap as such and **B** sediment and active cap with grinding. N/A means that the blank sample did not contain the metal in question, and thus the calculation of stabilization efficiency is not possible. The green and red colors indicate decreased and increased bioaccessibility, respectively. See Table S1 in supporting material for the concentrations at different steps

of the leaching tests are shown in Fig. 6. (Concentrations of metals at different leaching stages can be seen from Supplementary material, Table S1.) The results in Fig. 6 are expressed as the stabilization efficiency (Eq. 1). The negative values of the stabilization efficiency indicate that the addition of active cap has increased bioaccessibility or that the active cap material itself has released metals. In the last step of the leaching experiments (analysis of the solid residue), negative values indicate that there has been accumulation of the metal in the stable solid phase.

$$\text{Stabilization efficiency} = \frac{\text{Leaching from blank sample}\left[\text{mgL}^{-1}\right] - \text{Leaching from sample with active cap }\left[\text{mgL}^{-1}\right]}{\text{Leaching from blank sample}\left[\text{mgL}^{-1}\right]} \quad (1)$$

The total amounts of metals in the sediment were 11,050 mg kg^{-1} of Al, 81,800 mg kg^{-1} of Fe, 386 mg kg^{-1} of Ti, 682 mg kg^{-1} of Zn, 638 mg kg^{-1} of Ni, 17 mg kg^{-1} of Cr, and 41 mg kg^{-1} of Cu as reported in the previous study by the authors (Kutuniva et al. 2019). However, the metals are not evenly dispersed in all sections of the lake. As the amount of some metals, such as Cr and Cu, are relatively low, the readers are advised the see also the supporting information for Table S1, which contains the actual concentrations of metals from each leaching step in addition to the stabilization efficiency as shown in Fig. 6. In general, the results of the three-stage leaching experiments (Fig. 6) indicate good stabilization of Fe, Zn, Ni, and Cr upon the addition of active cap in all extraction stages (acidic, reducing, and oxidizing). On the other hand, the results of Al, Ti, and Cu are mixed, as in some extraction stages, the leaching increases in comparison with the sediment without active cap. The grinding of dried sediment with active cap further decreases the bioaccessibility of Al, Fe, and Ti, while Zn, Ni, Cr, and Cu remained unaffected. The improved immobilization of metals after grinding is likely due to the increased surface area as granules are crushed. In those cases when the solid residual had a concentration lower than the detection limit (e.g., Zn and Ni), the extraction treatments have likely removed all of the metals from the sediment (see supporting information, Table S1). The pH of the unamended sediment was 6.6, whereas the pH of sediment and active cap was 8.4. The increase in pH may contribute to the improved stability, but it may be also toxic to the benthic biota (Gu et al. 2019).

3.4 Sediment pore waters from mesocosm experiments

Pore water samples were collected from the mesocosm that was treated with both sediment augmentation and artificial mixing. The purpose of the mixing was to eliminate the saline mine water-induced stratification, as reported earlier (Karppinen et al. 2019; Mäkinen and Saarelainen 2020). The concentrations of P and As were lower in the pore waters of the mesocosms with induced circulation than in the sediments outside the mesocosm while with other elements (Table 4). In the case of water mixing causing the decrease in an element concentration, the mechanism might be related to the increase in redox potential. More variability was observed with the BFS-treated mesocosms in terms of the pore water concentrations of Al, As, Ca, Fe, Mg, Mn, and Ni than in the other two sediment types. In contrast, the pore water concentrations of K and P were higher in the BFS-treated mesocosm than outside the mesocosms or in the induced circulation mesocosm, especially in the second mesocosm location. However, the increased P content is not originating from the alkali-activated BFS since its P content is low (0.01 weight-% as P2O5). It might be a result of mixing and local pH variation upon active cap dosing. Nevertheless, the P increase does not appear to follow consistent trend as it is very minor on location 1 in comparison with location 2 (see Table 4).

In general, pore water concentrations of As, Fe, U, Zn, and DOC decreased during the 3-month incubation experiments (Table 5). In contrast, concentrations of Al, Ca, Mg, Mn, P, and S increased. Adding BFS on top of the sediment produced changes similar to the field setups with clearly decreased pore water concentrations of Ba, Co, Fe, Mg, Mn, and Ni, combined with increased concentrations of K, P, V, and Zn.

3.5 Discussion of the stabilization mechanisms of the studied metals

The stabilization of the metals in sediments by alkali-activated BFS occurs likely via several different mechanisms. As indicated by the zeta potential measurements, the granules contain both negatively (i.e., [AlO4]− in the framework of AAMs and surface Si–OH and Al–OH groups) and positively (i.e., layered double hydroxides) charged surface sites. Thus, granules can bind both negatively and positively charged ions from water.

Table 4 Surface sediment (0–5 cm) pore water metal concentrations in the mesocosm setups from two locations at Lake Kivijärvi in 2017. Pore waters were analyzed from sediments immediately outside of the mesocosms, in mesocosms where the stratification was disturbed by pumping, and in mesocosms with both pumping and a BFS layer

	Al µg L^{-1}	As µg L^{-1}	Mn µg L^{-1}	Ni µg L^{-1}	P µg L^{-1}	Zn µg L^{-1}	Ca mg L^{-1}	Fe mg L^{-1}	K mg L^{-1}	Mg mg L^{-1}
Outside (location 1)	317	0.2	36,200	7.6	333	7	130	67	6.5	141
Induced circulation (location 1)	176	< 0.05	27,600	0.7	189	14	105	83	6.1	112
BFS-treated (location 1)	195	0.1	32,600	2.6	338	7	122	62	6.5	132
Outside (location 2)	212	0.3	37,400	4.1	202	4	140	71	6.3	169
Induced circulation (location 2)	241	< 0.05	38,400	5.6	138	8	141	76	6.6	171
BFS-treated (location 2)	196	0.1	22,900	0.1	342	6	120	33	21.6	151

In addition, the presence of unreacted alkali-activator (i.e., NaOH) may induce local increase in pH and cause precipitation of some metals as hydroxides. However, as indicated by the sequential extraction experiments, metals were stable also at acidic conditions, which indicates that precipitation as hydroxides was not a major mechanism in stabilization. In the following, each metal is discussed in detail related to its possible stabilization mechanism.

Aluminum is sparingly soluble in the typical conditions of natural aqueous environments: $Al(OH)_3$ precipitates at pH > 4 but is re-dissolved at pH > 11 as $Al(OH)_4^-$ (Schweitzer and Pesterfield 2010). As pH may increase drastically in the immediate vicinity of BFS granules for a short period, it might be possible that anionic Al species were formed and adsorbed by the granules. The observed behavior of Al (Fig. 6) follows the same pattern that was reported in our previous work (Kutuniva et al. 2019): enhanced stabilization at acid extraction and reduction stages, even though the oxidation stage causes a significant release of Al compared to the sediment without active cap. It appears that the alkali-activated BFS is not stable in the highly oxidizing conditions, and it releases some of the Al it contains. Nevertheless, the extreme oxidizing conditions of the sequential leaching experiment are unlikely to occur in natural environment. However, the solid residual fraction clearly contained higher Al content compared to the blank. The three-month incubation experiments (Table 5) indicated only a minor increase (0.1 mg L^{-1}) of Al in the pore water due to the addition of alkali-activated BFS.

Iron can be present at + 2 or + 3 oxidation states, of which the first is soluble when pH is less than approximately 6 and the latter only when pH is less than approximately 3 (Schweitzer and Pesterfield 2010). However, Fe^{2+} is easily oxidized to Fe^{3+} if the sediment is not completely anoxic. The stabilization of iron was consistently effective in every leaching step, and the amount in the stable solid fraction increased in comparison with the blank sample (Fig. 6). Changes in pH level might affect the precipitation of Fe, but since Fe also remained stable

in the acid leaching step, the results indicate stable chemical adsorption.

Titanium release increased at the acidic and reducing extraction steps in comparison with blank, but stayed unchanged at the oxidizing step (Fig. 6). Since the blank sample did not contain Ti above the detection limit, it can be concluded that Ti was released from the alkali-activated BFS. The amount of Ti in BFS is approximately 0.6 weight-% (Kutuniva et al. 2019). The maximum concentration of dissolved Ti detected at acid and reducing extraction steps was 0.87 ± 0.26 mg L^{-1} (see Supplementary material, Table S1). Dissolved Ti exists for example as TiO^{2+} which is, however, stable only when pH < 1 (Schweitzer and Pesterfield 2010). Due to the refractory nature of many Ti-containing minerals, the concentrations of dissolved Ti in surface waters are low: commonly clearly lower than 100 µg L^{-1} (Linnik and Zhezherya 2015). However, in extreme cases, concentrations up to 1180 µg L^{-1} have been detected (Linnik and Zhezherya 2015). There is evidence that dissolved Ti is a reactive and short-residence-time element in the aquatic environment (Orians et al. 1990). The biological functions and toxicity of dissolved Ti appear to be unclear even though TiO_2 nanoparticles are known to be toxic (Das et al. 2013).

Zinc (concentration in the sediment is 682 mg kg^{-1}; Kutuniva et al. 2019) was found to be stabilized in a consistent manner at all leaching stages, but its amount was below the detection limit from the stable residue (see Fig. 6). This may reflect the fact that Zn species in the sediment are so labile that they are completely removed during the sequential extraction steps. Zn is present as dissolved Zn^{2+} in acidic conditions and precipitated $Zn(OH)_2$ in the pH region of approximately 6.5–12.5 (Schweitzer and Pesterfield 2010). However, its stabilization upon alkali-activated BFS addition was likely not due to the precipitation since Zn was not re-released at the acid extraction step.

Nickel (concentration in the sediment is 638 mg kg^{-1}; Kutuniva et al. 2019) behaved similarly to Zn: an effective stabilization was observed at all leaching stages, but the

Table 5 Elemental and DOC concentrations from the three-month incubation experiment: lake and pore waters initially and after the experiment with either sediment layer and lake water (INC) or sediment, BFS and lake water (INC+BFS)

	As µg L⁻¹	Ba µg L⁻¹	Co µg L⁻¹	Ni µg L⁻¹	P µg L⁻¹	U µg L⁻¹	V µg L⁻¹	Zn µg L⁻¹	Al mg L⁻¹	Fe mg L⁻¹	K mg L⁻¹	Mg mg L⁻¹	Mn mg L⁻¹	Na mg L⁻¹	S mg L⁻¹	DOC mg L⁻¹
Lake water, initially	0.7	46	5	3	588	4.9	8.0	6.06	0.4	58	6	149	35	1600	1470	41
Pore water, initially	1.06	54	7	39	229	4.3	8.1	8.72	0.4	57	7	144	33	1550	1450	37
Lake water, INC	<0.05	45	5	32	458	0.7	7.5	<0.2	0.9	28	8	160	37	1660	1700	18
Pore water, INC	0.28	55	11	65	372	0.6	6.2	<0.2	0.9	47	10	181	49	1760	1830	22
Lake water, INC+BFS	<0.05	33	2	41	98	1.0	7.9	7.49	0.0	0	21	48	0	1830	1560	-
Pore water, INC+BFS	<0.05	24	1	14	598	3.9	15.9	21.6	1.0	2	21	49	3	1770	1500	-

solid residue had a Ni content below the detection limit. Similarly as with Zn, likely all Ni species are extracted from the sediments during acidic, reducing, and oxidizing treatment steps. Ni exists as dissolved Ni2+ in aquatic environments but is prone to precipitate as Ni(OH)2 when the pH is higher than approximately 7 (Schweitzer and Pesterfield 2010). However, similar to Zn, the stabilization of Ni was not likely due to precipitation since it was not re-released at acid extraction. The stabilization of Ni would be important in the studied case, as it was released in a larger quantity, with a total 2 t of Ni (Kauppi et al. 2013; Leppänen et al. 2017), and it is known to be highly toxic in the aquatic environment (Liber et al. 2011).

Chromium (concentration in the sediment is 17 mg kg−1; Kutuniva et al. 2019) can be present in aqueous environments at oxidation states +3 (i.e., cationic Cr3+) or +6 (i.e., oxyanions such as CrO42−) (Schweitzer and Pesterfield 2010). In the present study, Cr was analyzed as the total Cr. The Cr content in the sediment without active cap was low (see Supplementary material, Table S1), but the addition of alkali-activated BFS still improved the stabilization at the reduction and oxidation leaching steps.

Copper (concentration in the sediment is 41 mg kg−1; Kutuniva et al. 2019) is most commonly occurring as dissolved Cu2+ in the aquatic environment when pH < 5 (Schweitzer and Pesterfield 2010). In the current experiments, Cu was stabilized with varying success. When using the whole granules (Fig. 6A), the Cu stabilization decreased at the acid extraction stage in comparison with the blank, while it was successful at other stages. However, when the granules were ground, Cu stabilization decreased at the reducing extraction stage, while other stages exhibited improved stabilization in comparison with blank. Nevertheless, the observed Cu concentrations in the leaching experiments were small: maximum 0.08 + 0.04 mg L−1 (see Supplementary materials, Table S1). BFS contains only trace amounts of Cu, and thus leaching of copper from BFS is not the reason for the observed behavior. However, alkali-activated BFS might exhibit lower selectivity for Cu2+ than for other cations.

3.6 Risk evaluation

The main risks involved in the present study are related to the use of BFS (by-product from iron/steel manufacturing) and the use of alkaline chemicals in the manufacturing of granules. On the other hand, the alkali activation of BFS may change the mobility of potentially toxic elements.

The concentrations of potentially toxic elements in BFS have been reported in the literature: median results of 53 samples showed that BFS contained 34 mg kg−1 of vanadium, 21.2 mg kg−1 of chromium, and 7.4 mg kg−1 of zinc (Matthes et al. 2018). In the same study, antimony, arsenic, lead, copper, molybdenum, and nickel were found to

be < 5 mg kg−1 and cadmium < 0.5 mg kg−1 (Matthes et al. 2018). On the other hand, the authors of the present study reported earlier that barium, beryllium, chromium, nickel and vanadium content of the BFS used in this study were 550, 4.6, 46, 1.2 and 410 mg kg−1, respectively (Kutuniva et al. 2019). In addition, phosphorus, lead, zinc, and tin were not detected (Kutuniva et al. 2019). Even though the aforementioned studies have reported the presence of certain potentially toxic elements in BFS, their mobility and bioavailability are hindered by the rapid cooling of molten slag, which results a glassy phase. This has been recently demonstrated in a study that showed no phenotypic changes in rats upon inhalation of BFS particles (Dillon et al. 2020). Another study showed that vanadium is sparingly available from BFS used for soil amendment (Larsson et al. 2015). In fact, the BFS used in the present study is routinely used as a liming material in agriculture in Finland.

Some of the alkaline chemicals used to prepare the granules (i.e., NaOH and sodium silicate) remain unreacted in the pore solution of alkali-activated BFS granules. They may leach out of the granules leading to increase in pH in water and minor increase in sodium cations. However, it is possible to neutralize the pore solution by performing pretreatment for alkali-activated materials before use (e.g., with 0.1 M acetic acid solution) (Szechyńska-Hebda et al. 2019; Selkälä et al. 2020). In the present study, this neutralization step was not performed, and thus pH increased from 6.6 to 8.4 in the sediment upon granule addition. However, as the experiment was conducted in a mesocosm, the mixing of water was limited leading to probably higher increase in pH compared to actual use scenario. Nevertheless, in the future studies and possible practical use, the neutralization step should be performed.

Finally, alkali activation may induce changes to mobility of the potentially toxic elements in BFS. Thus, a thorough evaluation of bioavailability of trace elements should performed for alkali-activated BFS. However, alkali activation using BFS as one potential binder precursor is widely studied as a solidification/stabilization method for different kinds of waste materials: in these studies, the mobility of potentially toxic elements decreases upon alkali activation (Shim et al. 2016; Koplík et al. 2018).

3.7 Cost evaluation

In this section, the material costs arising from the sediment augmentation with adsorbents at Lake Kivijärvi with alkali-activated BFS granules are provided to serve as an example of the cost of adsorbent augmentation treatment.

The estimated unit prices of the raw materials and energy are as follows: BFS 80 € t−1, sodium silicate solution 450 € t−1, sodium hydroxide solution 400 € t−1, water 1 € t−1, and electricity 0.1 € kWh−1. The mixing ratios of raw materials employed in granule manufacturing are provided in Sect. 2.1. Energy consumption was estimated by considering that the granulator machine has a power of 25 kW, and it takes 22 min to prepare 1 t of granules. Consequently, the material and energy cost of alkali-activated BFS granules is approximately 168 € t−1.

The surface area of Lake Kivijärvi is approximately 188 ha. In this calculation, it is assumed that the areas of the lake basin containing most of the contamination constitute approximately 20% (or 37.6 hectares) of the surface area. If it is estimated that a 5-cm depth of the sediment is treated with 2.5 weight-% of granules, the required adsorbent amount is approximately 470 t. When considering the abovementioned unit cost of granules, the cost of treatment would be approximately 79 000 €. This figure is likely clearly lower than the cost of sediment dredging and off-site treatment. The cost of dredging is approximately 6.5 € m−3 (Frittelli 2019), which would result in a total cost of 120 000 € in the present example.

4 Conclusions

The use of alkali-activated blast furnace slag granules was demonstrated as an augmentation material for metal-contaminated lake sediment remediation in a field experiment. The experiment took place at Lake Kivijärvi (Sotkamo, Finland), which is heavily affected by the failure of the gypsum pond dam of the nearby mine. The experiment was executed in a mesocosm from which samples were taken after two weeks of active cap application, and the performance was evaluated with a sequential leaching test and analyses of sediment pore waters. Effective and consistent stabilization in comparison with sediment without active cap was observed for Fe, Zn, Ni, and Cr. However, the granule precursor, blast furnace slag, released some Al in the oxidative leaching stage and Ti in the acid and reducing leaching stages. For Cu, the stabilization performance in the acid and reducing extraction steps appeared to depend on whether alkali-activated slag was used as granules or powder. The material cost of granules was estimated to be ~ 168 € t−1, which results in a total treatment cost of ~ 79 000 € for Lake Kivijärvi if an active cap is applied only to the deepest parts of the lake basin. Further experiments should, however, be conducted to evaluate the long-term performance of alkali-activated active caps.

Availability of data and material Data of the research is available upon request.

Code availability Not applicable.

Declarations

Conflict of interest The authors have no relevant financial or non-financial interests to disclose.

References

Alvarado JN, Hong SH, Lee CG, Park SJ (2020) Comparison of capping and mixing of calcined dolomite and zeolite for interrupting the release of nutrients from contaminated lake sediment. Environ Sci Pollut Res 27:15045–15056. https://doi.org/10.1007/s11356-020-08058-y

Bortnovsky O, Dedecek J, Tvaružková Z, Sobalík Z, Šubrt J (2008) Metal ions as probes for characterization of geopolymer materials. J Am Ceram Soc 91:3052–3057. https://doi.org/10.1111/j.1551-2916.2008.02577.x

Cagnin RC, Quaresma VS, Chaillou G, Franco T, Bastos AC (2017) Arsenic enrichment in sediment on the eastern continental shelf of Brazil. Sci Total Environ 607:304–316. https://doi.org/10.1016/j.scitotenv.2017.06.162

Calmano W, Hong J, Förstner U (1993) Binding and mobilization of heavy metals in contaminated sediments affected by pH and redox potential. Water Sci Technol 28:223–235. https://doi.org/10.2166/wst.1993.0622

Ciszewski D, Kubsik U, Aleksander-Kwaterczak U (2012) Long-term dispersal of heavy metals in a catchment affected by historic lead and zinc mining. J Soils Sediments 12:1445–1462. https://doi.org/10.1007/s11368-012-0558-1

Das P, Xenopoulos MA, Metcalfe CD (2013) Toxicity of silver and titanium dioxide nanoparticle suspensions to the aquatic invertebrate, Daphnia magna. Bull Environ Contam Toxicol 91:76–82. https://doi-org.pc124152.oulu.fi:9443/10.1007/s00128-013-1015-6

Dillon K, Jochims K, Gerigk U, Jost F, Kobesen H, Bialucha R (2020) No pathogenic responses in rat lung upon exposure to ground granulated blast furnace slag (GGBS). Inhal Toxicol 32:39–52. https://doi.org/10.1080/08958378.2020.1731023

Dixon KL, Knox AS (2012) Sequestration of metals in active cap materials: a laboratory and numerical evaluation. Remed J 22(2):81–91. https://doi.org/10.1002/rem.21312

European Union (2000) Directive 2000/60/EC of the European Parliament and of the Council of 23 October 2000 establishing a framework for Community action in the field of water policy. OJL 327:1–73

Finnish Environment Institute (2019) Pintavesien ekologinen ja kemiallinen tila [Ecological and chemical status of surface waters]. Available online: https://www.ymparisto.fi/pintavesientila Accessed 6 April 2021

Frittelli J (2019) Harbor Dredging: Issues and Historical Funding. Congressional Research Service and William S. Hein & Company, Washington, District of Columbia, USA. Available online: https://crsreports.congress.gov/product/pdf/IN/IN11133 Accessed 6 April 2021

Gu BW, Hong SH, Lee CG, Park SJ (2019) The feasibility of using bentonite, illite, and zeolite as capping materials to stabilize nutrients and interrupt their release from contaminated lake sediments. Chemosphere 219:217–226. https://doi.org/10.1016/j.chemosphere.2018.12.021

Guo X, Shi H (2017) Microstructure and heavy metal adsorption mechanisms of hydrothermally synthesized Al-substituted tobermorite. Mater Struct 50:245. https://doi.org/10.1617/s11527-017-1100-0

Kang K, Lee CG, Choi JW, Kim YK, P SJ, (2016) Evaluation of the use of sea sand, crushed concrete, and bentonite to stabilize trace metals and to interrupt their release from contaminated marine sediments. Water Air Soil Pollut 227:308. https://doi.org/10.1007/s11270-016-3028-3

Karppinen A, Hadzic M, Laamanen T, Turunen J, Leinonen K, Nilivaara-Koskela R (2019) Kerrostuneisuuden purkaminen turvallisesti [Safe remediation of stratification in waterbodies]. In: Laamanen T, Mäkinen J, Koivuhuhta A, Nilivaara-Koskela R, Karppinen A, Hellsten S (Eds.) Kaivosvesiä vastaanottavien vesistöjen hallinta ja kunnostaminen. KaiHali-hankkeen loppuraportti. [Management and remediation of water bodies receiving mine waters. Final report of KaiHali project]. Finnish Environmental Institute. Available online: http://hdl.handle.net/10138/305517 Accessed 6 April 2021

Kauppi S, Mannio J, Hellsten S, Nysten T, Jouttijärvi T, Huttunen M, Ekholm P, Tuominen S, Porvari P, Karjalainen A (2013) Arvio Talvivaaran kaivoksen kipsisakka-altaan vuodon haitoista ja riskeistä vesiympäristölle [Assessment of detriments and risks of gypsum pond failure at Talvivaara mine]. Finnish Environmental Institute. Available online: http://hdl.handle.net/10138/38465 Accessed 6 April 2021

Koplík J, Solný T, Kalina L, Másilko J (2018) Immobilization of Sr2+, Bi3+ and Zn2+ in Alkali-Activated Materials Based on Blast Furnace Slag and Fly Ash. Key Eng Mater 761:15–18. https://doi.org/10.4028/www.scientific.net/kem.761.15

Kutuniva J, Mäkinen J, Kauppila T, Karppinen A, Hellsten S, Luukkonen T, Lassi U (2019) Geopolymers as active capping materials for in situ remediation of metal (loid)-contaminated lake sediments. J Environ Chem Engineer 7:102852. https://doi.org/10.1016/j.jece.2018.102852

Laamanen T, Mäkinen J, Koivuhuhta A, Nilivaara-Koskela R, Karppinen A, Hellsten, S. (2019) Kaivosvesiä vastaanottavien vesistöjen hallinta ja kunnostaminen. KaiHali-hankkeen loppuraportti. [Management and remediation of water bodies receiving mine waters. Final report of KaiHali project]. Finnish Environmental Institute. Available online: http://hdl.handle.net/10138/305517 Accessed 6 April 2021

Larsson MA, Baken S, Smolders E, Cubadda F, Gustafsson JP (2015) Vanadium bioavailability in soils amended with blast furnace slag. J Hazard Mat 296:158–165. https://doi.org/10.1016/j.jhazmat.2015.04.034

Lecome I, Henrist C, Liegeois M, Maseri F, Rulmont A, Cloots R (2006) Microstructural comparison between geopolymers, alkali-activated slag cement and Portland cement. J Eur Ceram Soc 16:3789–3797. https://doi.org/10.1016/j.jeurceramsoc.2005.12.021

Leppänen JJ, Weckström J, Korhola A (2017) Multiple mining impacts induce widespread changes in ecosystem dynamics in a boreal lake. Sci Rep 7:1–11. https://doi.org/10.1038/s41598-017-11421-8

Liber K, Doig LE, White-Sobey SL (2011) Toxicity of uranium, molybdenum, nickel, and arsenic to Hyalella azteca and Chironomus dilutus in water-only and spiked-sediment toxicity tests. Ecotoxicol Environ Saf 74:1171–1179. https://doi.org/10.1016/j.ecoenv.2011.02.014

Linnik PN, Zhezherya VA (2015) Titanium in natural surface waters: The content and coexisting form. Russ J Gen Chem 85:2908–2920. https://doi.org/10.1134/S107036321513006X

Luukkonen T, Runtti R, Niskanen M, Tolonen E, Sarkkinen M, Kemppainen K, Rämö J, Lassi U (2016) Simultaneous removal of Ni (II), As (III), and Sb (III) from spiked mine effluent with metakaolin and blast-furnace-slag geopolymers. J Environ Manage 166:579–588. https://doi.org/10.1016/j.jenvman.2015.11.007

Luukkonen T, Heponiemi A, Runtti H, Pesonen J, Yliniemi J, Lassi U (2019) Application of alkali-activated materials for water and wastewater treatment: a review. Rev Environ Sci Biotechnol 18:271–297. https://doi.org/10.1007/s11157-019-09494-0

Luukkonen T, Sreenivasan H, Abdollahnejad Z, Yliniemi J, Kantola A, Telkki V, Kinnunen P, Illikainen M (2020) Influence of sodium silicate powder silica modulus for mechanical and chemical properties of dry-mix alkali-activated slag mortar. Constr Build Mater 233:117354. https://doi.org/10.1016/j.conbuildmat.2019.117354

Matthes W, Vollpracht A, Villagrán Y, Kamali-Bernard S, Hooton D, Gruyaert E, Soutsos M, De Belie N (2018) Ground Granulated Blast-Furnace Slag. In: De Belie N, Soutsos M, Gruyaert E. (eds) Properties of Fresh and Hardened Concrete Containing Supplementary Cementitious Materials. RILEM State-of-the-Art Reports. Springer, Cham. https://doi.org/10.1007/978-3-319-70606-1_1

Mehta A, Siddique R (2016) An overview of geopolymers derived from industrial by-products. Constr Build Mater 127:183–198. https://doi.org/10.1016/j.conbuildmat.2016.09.136

Myers RJ, Bernal SA, San Nicolas R, Provis JL (2013) Generalized structural description of calcium-sodium aluminosilicate hydrate gels: The cross-linked substituted tobermorite model. Langmuir 29:5294–5306. https://doi.org/10.1021/la4000473

Mäkinen J, Saarelainen J (2020) KaiHali-hankkeen taustaraportti [Background report for the KaiHali project]. Finnish Environment Institute. Available online: https://www.syke.fi/download/noname/%7B52BE3639-B2A4-49AC-A19F-6491065ECF78%7D/149669 Accessed: 6 April 2021

Orians KJ, Boyle EA, Bruland KW (1990) Dissolved titanium in the open ocean. Nature 348:322–325. https://doi.org/10.1038/348322a0

Park S, Kang K, Lee C, Choi J (2019) Remediation of metal-contaminated marine sediments using active capping with limestone, steel slag, and activated carbon: a laboratory experiment. Environ Technol 40:3479–3491. https://doi.org/10.1080/09593330.2018.1478886

Parker LM, Milestone NB, Newman RH (1995) The use of hydrotalcite as an anion absorbent. Ind Eng Chem Res 34:1196–1202. https://doi.org/10.1021/ie00043a023

Provis JL (2014) Introduction and scope. In: Provis JL, Van Deventer JSJ (eds) Alkali Activated Materials, State-of-the-Art Report. RILEM TC 224-AAM. Springer, Dordrecht, pp 1–9. https://doi.org/10.1007/978-94-007-7672-2_1

Provis JL, Bernal SA (2014) Geopolymers and related alkali-activated materials. Annu Rev Mater Res 44:299–327. https://doi.org/10.1146/annurev-matsci-070813-113515

Randall PM, Yates BJ, Lal V, Darlington R, Fimmen R (2013) In-situ subaqueous capping of mercury-contaminated sediments in a freshwater aquatic system, Part II-evaluation of sorption materials. Environ Res 125:41–51. https://doi.org/10.1016/j.envres.2013.03.010

Rauert G, Lopez-Sanchez JF, Sahuquillo A, Rubio R, Davidson C, Ure A, Quevauviller P (1999) Improvement of the BCR three step sequential extraction of new sediment and soil reference materials. J Environ Monit 1:57–61. https://doi.org/10.1039/A807854H

Salomons W, Stigliani WM (2012) Biogeodynamics of Pollutants in Soils and Sediments: Risk Assessment of Delayed and Non-Linear Responses. Springer Science & Business Media, Germany

Saup CM, Williams KH, Rodríguez-Freire L, Cerrato JM, Johnston MD, Wilkins MJ (2017) Anoxia stimulates microbially catalyzed metal release from Animas River sediments. Environ Sci Process Impacts 19:578–585. https://doi.org/10.1039/C7EM00036G

Selkälä T, Suopajärvi T, Sirviö JA, Luukkonen T, Kinnunen P, de Carvalho ALCB, Liimatainen H (2020) Surface modification of cured inorganic foams with cationic cellulose nanocrystals and their use as reactive filter media for anionic dye removal. ACS Appl Mater Interfaces 12:27745-27757. https://doi.org/10.1021/acsami.0c05927

Schweitzer GK, Pesterfield LL (2010) The Aqueous Chemistry of the Elements. Oxford University Press, USA

Szechyńska-Hebda M, Marczyk J, Ziejewska C, Hordyńska N, Mikuła J, Hebda M (2019) Optimal design of pHneutral geopolymer foams for their use in ecological plant cultivation systems. Materials 12:2999. https://doi.org/10.3390/ma12182999

Shim JH, Jeong JY, Park JY, Ryu JS, Park JY (2016) Characterization of alkali-activated slag paste containing dredged marine sediment. Desalin Water Treat 57:24688–24696. https://doi.org/10.1080/19443994.2016.1157993

Ting Y, Chen C, Ch'ng B, Wang Y, His H (2018) Using raw and sulfur-impregnated activated carbon as active cap for leaching inhibition of mercury and methylmercury from contaminated sediment. J Hazard Mater 354:116–124. https://doi.org/10.1016/j.jhazmat.2018.04.074

Ting Y, His H (2019) Iron sulfide minerals as potential active capping materials for mercury-contaminated sediment remediation: a minireview. Sustainability 11:1747. https://doi.org/10.3390/su11061747

Trifiro F, Vaccari A (2004) Handbook of Layered Materials. CRC Press, USA

Viana PZ, Yin K, Rockne KJ (2008) Modeling active capping efficacy. 1. Metal and organometal contaminated sediment remediation. Environ Sci Technol 42:8922–8929. https://doi.org/10.1021/es800942t

Zhang C, Zhu M, Zeng G, Yu Z, Cui F, Yang Z, Shen L (2016) Active capping technology: a new environmental remediation of contaminated sediment. Environ Sci Pollut Res 23:4370–4386. https://doi.org/10.1007/s11356-016-6076-8